



# Shape memory behaviors in a $\text{Ti}_{50}\text{Ni}_{33.5}\text{Cu}_{12.5}\text{Pd}_4$ alloy with near-zero thermal hysteresis

Hang Li <sup>a, b</sup>, Xianglong Meng <sup>a, \*</sup>, Wei Cai <sup>a</sup>

<sup>a</sup> National Key Laboratory Precision Hot Processing of Metals, Harbin Institute of Technology, Harbin 150001, People's Republic of China

<sup>b</sup> School of Materials Science and Engineering, Heilongjiang University of Science and Technology, Harbin 150027, People's Republic of China



## ARTICLE INFO

### Article history:

Received 25 April 2018

Received in revised form

15 June 2018

Accepted 18 June 2018

Available online 19 June 2018

### Keywords:

Ti-Ni-Cu-Pd alloy

Shape memory alloys (SMAs)

Martensitic phase transformation

Shape memory effect (SME)

## ABSTRACT

The shape memory behaviors and the hysteresis under load in a  $\text{Ti}_{50}\text{Ni}_{33.5}\text{Cu}_{12.5}\text{Pd}_4$  alloy with near-zero thermal hysteresis have been investigated. There exists a deviation between the loaded and stress-free hysteresises. The recoverable strain increases with increasing the applied strain for the present alloy. The plastic strain can be detected when the applied strain is over 3%. The shape memory effect and hysteresis show excellent stability during the thermal cycling when the external stress is applied, which should be attributed to the extreme difficulty of dislocation introduction.

© 2018 Elsevier B.V. All rights reserved.

## 1. Introduction

Shape memory alloys (SMAs) have attracted much interest due to the unique shape memory effect and multi phenomena of martensitic transformation. In recent years, the most extensively studied SMAs are: TiNi- [1–4], Cu- [5], Fe-base [6] and NiMnGa-base [7] SMAs. Among these types of performance materials, Ti-Ni SMAs have enormous advantages such as large recovery stress and recoverable deformation [8–12]. Whereas, the temperatures hysteresises of the phase transformation are about 20–40 °C in Ti-Ni alloys, followed by the slow response speed and low sensitivity in actuator drives. Besides, the functional properties decay with the increase of the thermal cycles in the working state. After the thermal cycling, the martensite transformation beginning temperature ( $M_s$ ) reduces 30 °C in Ti-Ni alloys due to the introduction of the dislocations, which lead to the deterioration of the functional properties in actuator drives [13,14]. Presently, it has been found that Ti-Ni-Cu-Pd alloys show not only narrow hysteresis, but also high thermal stability, which means the phase transformation temperatures of Ti-Ni-Cu-Pd alloys almost do not shift during the thermal cycling [15,16]. However, the hysteresises of Ti-Ni-Cu-Pd alloys are measured by differential scanning calorimetry (DSC)

and alternating current potential drop method (ACPD) in a stress-free situation. The SMA actuators usually work under an external load, such as a bias spring in the slideable shutter. In that case, the hysteresis and its stability are different from that in the stress-free condition [17,18]. For example, in the solution-treated  $\text{Ti}_{50}\text{Ni}_{35}\text{Cu}_{15}$  alloy, the loaded hysteresis is 7 °C while the stress-free one is 9.5 °C. The shape recovery and hysteresis under load play very important roles on the application for SMAs. Therefore, the purpose of the present research is to investigate the hysteresis and shape memory behavior of a  $\text{Ti}_{50}\text{Ni}_{33.5}\text{Cu}_{12.5}\text{Pd}_4$  alloy with a near-zero hysteresis under load. Furthermore, the mechanisms of the loaded hysteresis and high stability of shape memory effect are discussed.

## 2. Experimental

The alloys were prepared with high purity elements by melting 10 times under argon atmosphere in an arc furnace with nominal composition of  $\text{Ti}_{50}\text{Ni}_{33.5}\text{Cu}_{12.5}\text{Pd}_4$  (at.%). The specimens were annealed in vacuum quartz tubes at 950 °C for 7.2 ks, and then water-quenched. The phase transformation temperatures were determined by the Perkin-Elmer diamond differential scanning calorimetry (DSC) to be  $M_f = 34.2$  °C;  $M_s = 37.7$  °C;  $A_s = 38.7$  °C;  $A_f = 42.2$  °C, with a cooling/heating rate of 10 °C/min. By linear fitting of the DSC results with different scanning rates, the hysteresis is 2.1 °C when the scan rate gets close to zero. The lattice parameters were determined through X-ray diffraction (XRD)

\* Corresponding author.

E-mail address: [xlmeng@hit.edu.cn](mailto:xlmeng@hit.edu.cn) (X. Meng).

measurements using an X' Pert PRO MPD with Cu K $\alpha$  radiation at 50 mA and 50 kV, with a scanning rate of 10°/min: for B2 phase,  $a = 0.3036$  nm; for B19 martensite,  $a = 0.2884$  nm,  $b = 0.4296$  nm,  $c = 0.4521$  nm. The tensile tests were performed on an Instron-5569 type electronic universal mechanical testing machine with a deformation rate of 1%/min, and the size of the samples was  $1 \times 1 \times 50$  mm with a gauge length of 20 mm. A new specimen was used for each tensile test. The alloys were heated to 100 °C after deformation to see the shape memory effect. The tensile strain-temperature measurements were performed on a Q800 type dynamic thermomechanical analysis machine with a deformation rate of 1%/min, and the size of the samples was  $0.2 \times 0.5 \times 50$  mm with a gauge length of 20 mm. This test involved loading a sample at a high temperature, cooling it to  $-20$  °C at a rate of 2 °C/min and reheating it to the original temperature at a rate of 2 °C/min. A series of strain-temperature measurements under various constant stresses was carried out. An FEI TECNAI G2 20 STWIN 300 kV transmission electron microscope (TEM) equipped with a double-tilt cooling stage was used for microstructure observation at room temperature. Specimens for transmission electron microscopy (TEM) observation were first mechanically polished to about 70  $\mu$ m then twinjet electropolished holding by a copper collar using a solution containing 10% perchloric acid and 90% ethyl alcohol (by volume). The temperature during twinjet electropolishing was  $-20$  °C.

### 3. Results and discussions

The tensile stress-strain curves of  $\text{Ti}_{50}\text{Ni}_{33.5}\text{Cu}_{12.5}\text{Pd}_4$  alloy under different applied strains are shown in Fig. 1a–e. The dotted lines represent the recovery strain after heating to 100 °C for 1 min. It can be seen that the curve can be divided into several stages. The first is a linear stage corresponding to the elastic deformation of martensitic phase in the alloy. After the first linear stage, there is a short stress plateau in the stress-strain curve, which is similar to Ti-Ni-Cu alloys [19]. Such a stress plateau indicates the reorientation of B19 martensite variants, which occurs via the movement of internal twin boundaries and eventually creates new twins. For the present alloy, the strain can recover completely when the strain is

less than the stress plateau. After the stress plateau, the stress increases rapidly with the increase of the strain again. In this stage, along with the increase of the prestrain, the residual strain gradually increases, just as the same as the recovered strain. The effect of the applied strain on the recoverable strain and the plastic strain of  $\text{Ti}_{50}\text{Ni}_{33.5}\text{Cu}_{12.5}\text{Pd}_4$  alloy are shown in Fig. 1f  $\epsilon_r$  and  $\epsilon_p$  in the graph represent the recoverable and plastic strain, respectively. It shows a complete recoverable strain of 2% and a maximum recovered strain of 4.9% under 6% applied strain in the present alloy. The Bain matrix associated with the transformation between B2 parent phase and B19 martensite is:

$$B = \begin{bmatrix} \lambda_1 & 0 & 0 \\ 0 & \lambda_2 & 0 \\ 0 & 0 & \lambda_3 \end{bmatrix} \quad (1)$$

Thereinto,  $\lambda_1 = a/a_0$ ;  $\lambda_2 = b/\sqrt{2}a_0$ ;  $\lambda_3 = c/\sqrt{2}a_0$ .  $a_0$  is the lattice parameter of B2 parent phase;  $a$ ,  $b$  and  $c$  are the lattice parameters of orthorhombic B19 martensite. The largest recoverable strain of the phase transformation can be estimated as  $(\lambda_3 - 1) \times 100\%$  [20]. In the present alloy, the calculated value is 5.3%. The difference between the calculated value and the measurement one is similar to that in Ti-Ni-Cu alloys, which is probably because the former is calculated based on the ideal single crystal structure, and the latter is obtained by experiment on the polycrystalline sample [17,20].

Fig. 2 shows a series of stress-strain curves obtained at various temperatures for  $\text{Ti}_{50}\text{Ni}_{33.5}\text{Cu}_{12.5}\text{Pd}_4$  alloy. It can be seen that there are stress plateaus in all the stress-strain curves at temperatures from 25 °C to 80 °C. And the yield stress corresponding to the stress plateau increases with increasing deformation temperature. The relationship curve between the yield stress corresponding to the stress plateau and the deformation temperature of the tensile testing at different temperatures in  $\text{Ti}_{50}\text{Ni}_{33.5}\text{Cu}_{12.5}\text{Pd}_4$  alloy is plotted in Fig. 3a. As shown in the figure, the yield stress increases with the increasing tensile temperature. The relationship conforms to the Clausius-Clapeyron equation:

$$\frac{d\sigma}{dT} = \frac{\Delta H^{M-P}}{T_0 \epsilon} \quad (2)$$

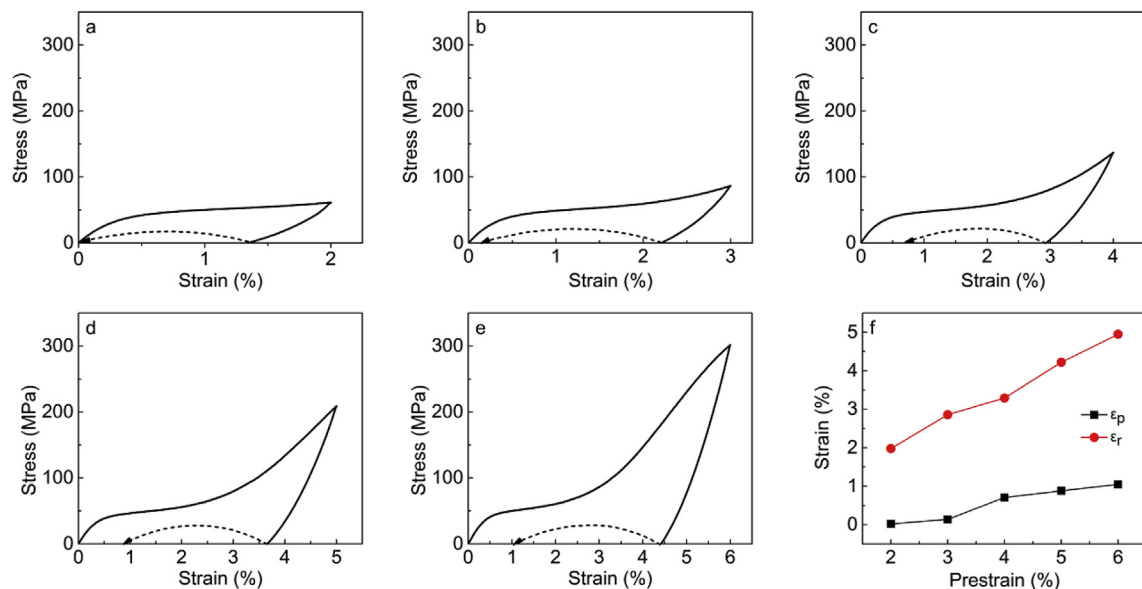


Fig. 1. (a–e) The tensile stress-strain curves of  $\text{Ti}_{50}\text{Ni}_{33.5}\text{Cu}_{12.5}\text{Pd}_4$  alloy under different applied strains. (f) The effect of the applied strain on the recoverable strain and the plastic strain.

Download English Version:

<https://daneshyari.com/en/article/7990476>

Download Persian Version:

<https://daneshyari.com/article/7990476>

[Daneshyari.com](https://daneshyari.com)